Available online at www.sciencedirect.com
ScienceDirect
Journal of Photochemistry and Photobiology A: Chemistry 186 (2007) 242–247
Journal of Photochemistry and Photobiology A:Chemistry
www.elsevier.com/locate/jphotochem

$CuAlO_2/TiO_2$ heterojunction applied to visible light H_2 production

R. Brahimi [a], Y. Bessekhouad [a,b,*], A. Bouguelia [a], M. Trari [a]

[a] *Faculty of Chemistry, USTHB, BP 32, El-Alia, Bab-Ezzouar, Algiers, Algeria*
[b] *National Veterinary School, BP 161-El Harrach, Algiers, Algeria*

Received 4 May 2006; received in revised form 23 July 2006; accepted 18 August 2006
Available online 30 August 2006

Abstract

$CuAlO_2/TiO_2$ heterojunction was prepared and studied for its potential application as dispersed photoelectrode capable to generate H_2 under visible light. Transport properties of delafossite $CuAlO_2$, i.e. thermoelectric power and electrical conductivity were studied and correlated to an optical and photoelectrochemical characterization to establish energetic diagram of the heterosystem $CuAlO_2/TiO_2$. The valence and the conduction bands were estimated to be respectively of −0.05 and of −1.34 V/SCE, which permit electron injection from activated $CuAlO_2$ to an activated TiO_2. This fact permitted a physical separation of charge carriers. Photocatalytic experiment performed using S^{2-} and $S_2O_3^{2-}$ showed efficiency respectively of 5265 and 60 μmol and then after 40 min of irradiation by visible light. The ideal heterojunction composition was $CuAlO_2$ (300 mg)/TiO_2 (75 mg). In all cases, the heterosystem was found to be more efficient than $CuAlO_2$ alone whatever the conditions. The optimal pH value was estimated to be of 11.

Keywords: Heterojunction; $CuAlO_2$; TiO_2; H_2-photoproduction; Delafossite

1. Introduction

Solar hydrogen production using semiconductor (SC) materials continue to attract much attention since the first reports on this innovation in the beginning of the 1970s [1–3]. As it is well admitted, hydrogen energy is one of the most serious candidates to replace the fossil fuel [4]. In addition, hydrogen is renewable, it possesses one of the highest energy capacity per unit mass and does not produce any pollutant during combustion [5]. The development of water photoelectrolysis technology is intimely connected to the development of materials [6]. Two types of materials are usually used for such applications: (i) wide band gap SC such as TiO_2, which has the advantage of high stability toward photocorrosion and can split water simultaneously into H_2 and O_2. However, they absorb only the UV light and are of little practical use in regard to solar emission, which contain less than 4% of UV irradiation. (ii) Narrow band gap SC such as CdS absorbs visible light and is very attractive for solar energy conversion. Nevertheless, this type of SCs has commonly a subject of photocorrosion and is challenged to be stabilised for long term of utilisation in aqueous electrolytes.

Recently, very interesting SC crystallizing in the delafossite structure ($CuAlO_2$) has been developed for solar to hydrogen conversion under visible light [7]. $CuAlO_2$ is a very stable material, even in strong acidic electrolytes such as HCl, $HClO_4$ or aqua regia and then for long periods of time. Preliminary investigations of $CuAlO_2$ properties and photocatalytic performance showed that this material is able to generate hydrogen under visible light. However, their performances remain moderated and suffer of a charge carrier lost by recombination and then even by using holes scavenger such as S^{2-} or $S_2O_3^{2-}$ [7].

Noble metal or noble metal oxide such Pt, Au, Ag and RuO_2 are commonly used to prevent charge carrier recombination by their act as electron accumulators which facilitate charge separation and electron transfer [8–10]. However, it should be noted that these materials are costly and they are not easily recovered after use. Recently, some heterojunctions based on the coupling of narrow and wide band gap SCs have been developed [11,12]. The synergy between the properties of each group of materials resulted on an increasing of photocatalytic activity of composite materials under visible illumination [13,14]. The physic that takes place for this photoelectrode configuration can be applied for an oxidation process (advanced oxidation process (AOP)),

* Corresponding author at: Faculty of Chemistry, USTHB, BP 32, El-Alia, Bab-Ezzouar, Algiers, Algeria. Tel.: +213 21 24 79 50; fax: +213 21 24 73 11.
E-mail address: ybessekhouad@yahoo.com (Y. Bessekhouad).

1010-6030/$ – see front matter © 2006 Elsevier B.V. All rights reserved.
doi:10.1016/j.jphotochem.2006.08.013

as well as for a reduction process (H_2 photoproduction from water).

The aim of this work is to progress our knowledge on some physico-chemical properties of $CuAlO_2$ and to improve its photocatalytic performance by their use in the presence of TiO_2.

2. Experimental

2.1. Heterojunction preparation

$CuAlO_2$ was prepared by dissolving stoichiometric amounts of $Al(NO_3)_3{\cdot}9H_2O$ (Merck, >98%) and CuO (Riedel-deHaën, 98%) in concentrated HNO_3 solution. The obtained solution was dehydrated by heating over flame until it became a black precipitate. After grinding in mortar, the powder was calcined at 900 °C for 18 h. TiO_2 was purchased from Degussa (TiO_2-P25) and used as received. The heterojunction $CuAlO_2/TiO_2$ was obtained by directly mixing both catalysts during photocatalytic experiment.

2.2. Materials characterization

Powder X-ray diffraction (XRD) patterns of $CuAlO_2$ and TiO_2 were obtained with a Philips diffractometer equipped with a monochromated high intensity Cu Kα in the scan range 2θ between 20° and 80°.

Absorption and reflectance spectra of pure SCs were recorded with a Cary 500 UV-VIS-NIR spectrophotometer equipped with an integrated sphere. $BaSO_4$ was used as a reference to measure all samples. The spectra were recorded at room temperature in air in the range of 300–2000 nm enabling the study of the spectral properties of these materials.

The transport properties of $CuAlO_2$ were studied by measuring the dc electrical resistivity ρ by the two-terminal method and the thermopower data S ($=\Delta V/\Delta T$) were obtained using an equipment described elsewhere [15]. $CuAlO_2$ was used in the form of compactness-sintered pellets heated in the same conditions as their preparation. A compactness of 83% was obtained.

Electrochemical measurements were performed in 1 M KOH (pH 13) using a "three electrode device": the $CuAlO_2$, a large platinum counter electrode and a saturated calomel reference electrode (SCE) to which all potentials were quoted. The electrolyte was continuously flushed with pure nitrogen gas. The intensity–potential $J(V)$ characteristics were recorded with a PRT 20-2X Tacussel potentiostat. A 200 W Oriel (model 66183) tungsten–halogen lamp was used as a light source. The light intensity of 74 mW cm^{-2} was estimated by a light-meters to attain the surface of the working electrode.

Photocatalytic experiments were carried out in a closed system equipped with a Pyrex double wall reactor connected to a thermostatic bath, whose temperature was fixed at 50 ± 0.1 °C. The closed system was connected to a water manometer. The detailed assembly was reported previously [16]. Typically for each experiment, powder catalyst is suspended by magnetic stirring in 200 ml of aqueous S^{2-} or $S_2O_3{}^{2-}$ (0.025 M) solution and submitted to three tungsten lamps each one of 200 W. Prior to irradiation, the mixture is flushed with N_2 for 30 min to remove dissolved oxygen from the electrolyte. Qualitative H_2 identification has been made using gas chromatography techniques in which a molecular sieve 13× column and an Ar as gas carrier were used.

3. Results and discussion

The X-ray powder pattern of $CuAlO_2$ revealed a well-crystallized single phase with the space group $R3m$, according to the JSPDS No. 35-1401. The unit cell parameters ($a = 0.2855$ nm and $b = 1.6947$ nm) are in good agreement with our previous results [7]. The crystallite size was determined according to the Scherrer equation using the full-width at half-maximum (FWHM) of the peak presenting the highest intensity (0 2 1). The crystallite size was estimated to be 29 nm. This value is smaller than that obtained for $CuAlO_2$ prepared by a solid-state reaction at 1150 °C [7]. The XRD pattern of commercial TiO_2-P25 reveled, as it is well known a mixture of anatase and rutile phases with a major composition on anatase.

Diffuse reflectance spectroscopy was used to determine the optical properties of pure $CuAlO_2$. Indeed, the band gap was determined by plotting $(\alpha h\nu)^n$ versus $h\nu$ and extrapolating the linear portion which intercept the energy axes $h\nu$. α is the absorption coefficient, which depend on the wavelength, n can take the value 1/2 or 2, respectively, for indirect and direct optical transition. It should be noted that α is proportional to $\ln[(R_{max} - R_{min})/(R - R_{min})]$, where reflectance decreased from R_{max} to R_{min} due to the semiconductor absorption. R is the intermediate for any intermediate energy photons [17]. As presented in Fig. 1, indirect optical transition was observed at 1.29 eV and corresponds to the band gap energy. This value is inferior to that observed by others by about 0.4 eV [7,18] probably due to the decreasing of the particle size, generated from the preparation method which can induce an optical shifting of the band gap [19]. This result suggested that $CuAlO_2$ (1.29 eV) is more adequate for solar light harvesting contrary to TiO_2, which possesses a band gap of 3.2 eV as it is well known.

The study of the thermopower effect demonstrates that $CuAlO_2$ is p-type SC due to the positive coefficient $S_{303\,K}$

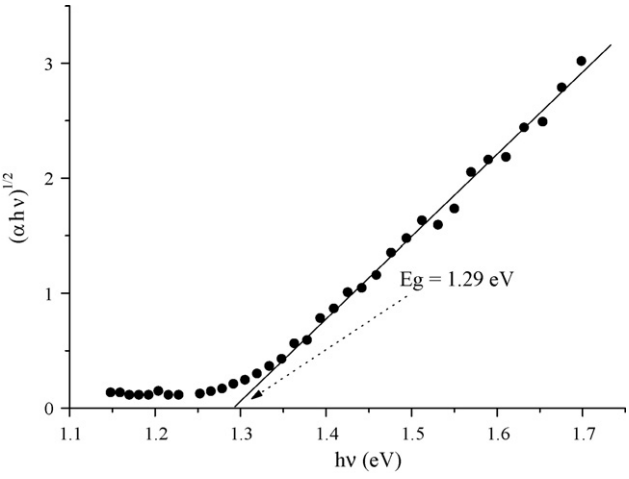

Fig. 1. Indirect band gap transitions of $CuAlO_2$.

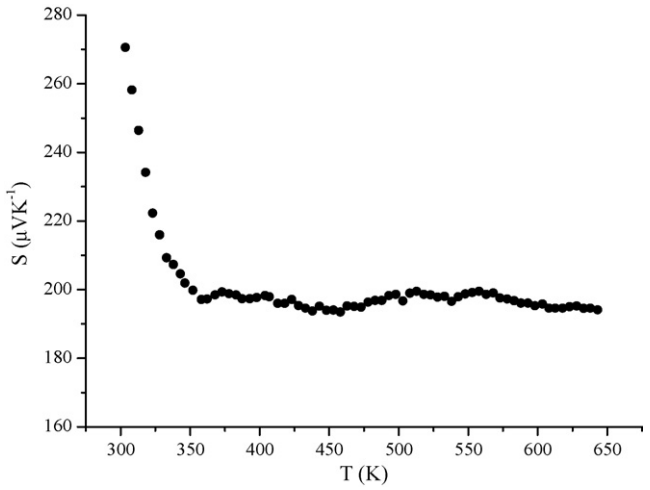

Fig. 2. Temperature dependence of thermopower (S) of $CuAlO_2$.

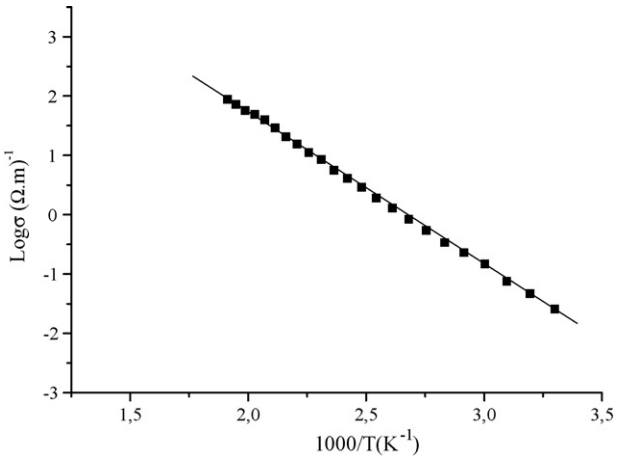

Fig. 3. Temperature dependence of the conductivity (σ) of $CuAlO_2$.

(270.60 μV K^{-1}) (Fig. 2). This type of conductivity is typical for $CuMO_2$ SC in which a small amount of oxygen is usually intercalated into the host layered lattice. This implies a limited generation of Cu^{2+} as required by the charge compensation mechanism and imposed by the delafossite structure. The thermal variation of S indicates that the conductivity is assumed by small hopping polarons between $Cu^{+/2+}$ ions mixed valences (i.e. Cu sites), which is traduced by a low value of activation energy ($\Delta E_S = 0.008$ eV). ΔE_S was determined according to the following equation that can be applied for such a mechanism:

$$S = \frac{k}{e}\frac{\Delta E_S}{kT} = \frac{k}{e}\ln\left(\frac{N_0}{N_A}\right)$$

N_0 and N_A are respectively the density of unoccupied and occupied polarons sites. The low ΔE_S value indicates that all charge carriers are ionized at room temperature and participate to the conduction. In this regard, small polarons have high concentration and low mobility. Some physical properties of $CuAlO_2$ are reported in Table 1.

The plotting of the $\log\sigma$ versus $1000/T$ shows that the electrical conductivity follows an Arrhenius law: $\sigma = \sigma_0 e^{-\Delta E/kT}$. $\Delta E_\sigma = 0.26$ eV is obtained from the slope of the linear portion (Fig. 3).

Photoelectrochemical characterization was performed in the aim to determine the flat band potential (V_{fb}) and to confirm the p-type character of $CuAlO_2$, elucidated from the $J(V)$ curves both in the dark and under illumination (Fig. 4). The apparition of the photocurrent J_{ph} started at a potential V_{ON} of −0.13 V and increased towards cathodic direction, which is typical of p-type behavior. It was also observed that J_{ph} increased slowly without reaching a limited potential value. This fact is attributed to the high resistivity of the electrode in which, under illumination, a large part of created charges are lost by trapping at grain boundaries. The potential V_{ON} can be reasonably considered as the potential (V_{fb}) that correspond to the position of the valence band for highly doped SC. It should be noted that V_{fb} was found insensitive to pH variation, which indicates that the valence band does not derive from deep oxygen O 2p generally observed for most oxides such as TiO_2 and $SrTiO_3$. Nevertheless, the valence band position of $CuAlO_2$ can be predicted using the known equation [20]:

$$E_{VB} = 4.75 + eV_{fb} + 0.059(\text{pH} - \text{pH}_{pzzp}) + \Delta E_S$$

pH_{pzzp} is the pH at the point of zero zeta potential (pzzp) and was found to be 7.75, ΔE_S is the activation energy and correspond to the separation between the Fermi level and the valence band that is determined from the thermoelectric power measurement. The valence band was located at 5.01 ± 0.1 eV below vacuum, a value in good agreement with that obtained for isostructural

Table 1
Some physico-chemical properties of $CuAlO_2$

E_g (eV)	1.29
V_{fb} (V)	−0.13
σ (Ω m)$^{-1}$	0.203
α (μV K^{-1})	270.6
N_0 (cm^{-3})	2.502×10^{22}
N_A (cm^{-3})	1.09×10^{21}
N_m (cm^{-3})	2.75×10^{21}
ΔE_σ (eV)	0.26
ΔE_S (eV)	0.08

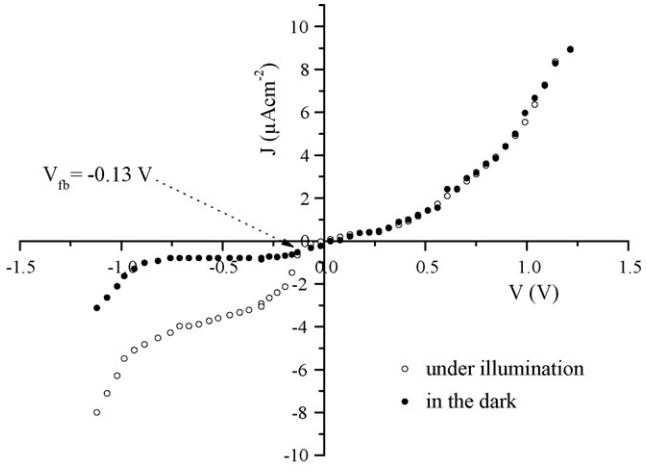

Fig. 4. $J(V)$ characteristics of $CuAlO_2$/1 M KOH/Pt plotted in the dark and under illumination with a scan rate of 3 mV/S.

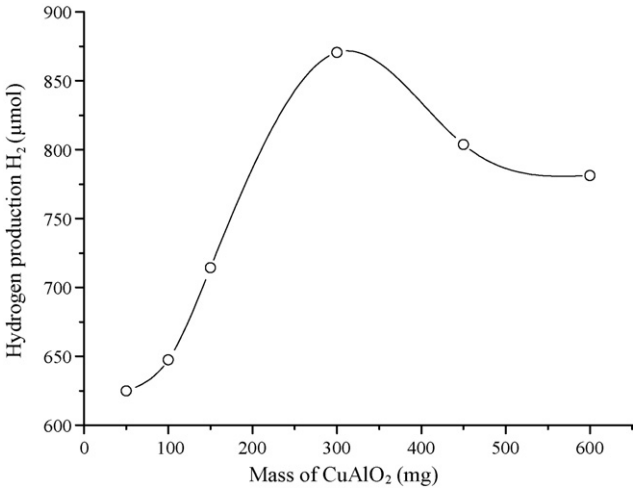

Fig. 5. H_2-amount toward $CuAlO_2$ mass in S^{2-} (0.025 M) electrolyte at pH ∼ 13.

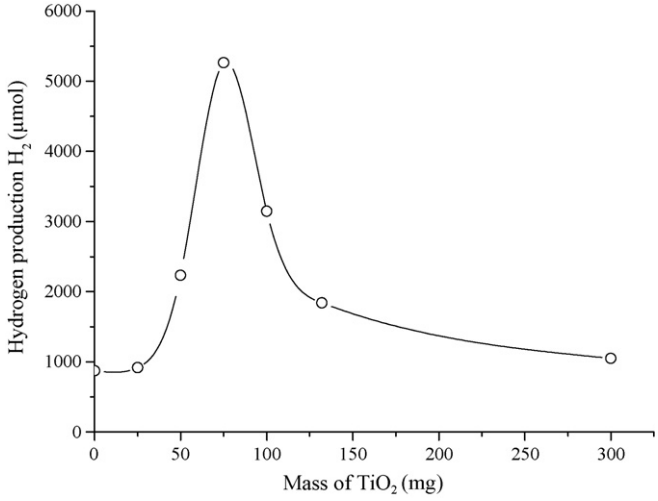

Fig. 6. H_2-amount toward TiO_2 mass in S^{2-} (0.025 M) electrolyte at pH∼13, the mass of $CuAlO_2$ (300 mg) was kept constant.

oxides for instance $CuMnO_2$ and $CuYO_2$ [20,21]. The case of ternary oxide ($Cu^{I+}M^{III+}O_2$) crystallized in delafossite structure is singular as well as attractive due to the fact that the valence band is made mainly from Cu 3d orbitals. This property leads to suitable applications of these SCs to water photoelectrolysis, in particular because of the H_2O/H_2 potential can be well matched to the conduction band through the pH variation.

3.1. Photoactivity

Fig. 5 shows the hydrogen production under illumination of pure $CuAlO_2$ suspended in S^{2-} solutions at different concentrations of the catalyst. It should be noted that the amount of H_2 production was taken after 40 min of irradiation above which a saturation plateau is reached. The saturation is induced by the competitive reduction of end products ($S_n{}^{2-}$, $2 \leq n \leq 5$) and the shift of H_2O/H_2 potential along cathodic direction. Before 40 min, a linear evolution of H_2 is observed. At first sight, H_2 production increased drastically with increasing catalyst concentration until to attain a maximum volume (870.53 μmol) for a catalyst concentration of 1.5 g/l, above which a decrease in the photoactivity is observed. The increasing of H_2 production is attributed to the increasing of the catalyst amount in which each particle, attained by photons, participates to the creation of charge carriers and accordingly increases the process of oxidation and reduction. When the concentration reached a critical value, the excess of the catalyst acts as an optical filter and in this regard, the particles become inactive. Further problems that can occur include the fact that inactivated particles can act as an electron–hole trapping system, inducing charge lost by recombination. These phenomenons are traduced, in our case, by decreasing H_2 production for catalyst concentration greater than 1.5 g/l. The best catalyst concentration (1.5 g/l) was selected to investigate photocatalytic performance of $CuAlO_2/TiO_2$ heterojunction.

Fig. 6 shows the photocatalytic activity of $CuAlO_2/TiO_2$ in which the mass of $CuAlO_2$ was maintained constant (300 mg) whereas that of TiO_2 varies between 0 and 300 mg. The amount of H_2 production was taken at the referenced time that is to say after 40 min of irradiation. As observed in Fig. 6, the addition of an appropriate amount of TiO_2 is very beneficial for improving H_2 production that means photocatalytic conversion efficiency. The maximum conversion efficiency was obtained for 75 mg of TiO_2 in which 5265 μmol of H_2 was obtained. This efficiency is six-fold greater than that obtained for pure $CuAlO_2$. Excess of TiO_2 induced a drastic decrease of conversion efficiency. However, this fact cannot be ascribed to the formation of an optical filter, since TiO_2 is completely transparent to visible light. Nevertheless, it should be taken into account that TiO_2 possesses a large resistivity and the loss of generated charges during the photocatalytic process is highly envisaged.

3.2. Photocatalytic process

The catalytic process taking place for pure $CuAlO_2$ and $CuAlO_2$ loaded TiO_2 under visible irradiation can be presented as follows: when $CuAlO_2$ is activated under visible light electron (e^-), hole (h^+) pairs are generated and subsequently separated by the junction electric field developed across the depletion layer. The electrons and holes migrate in opposite directions according to the p-type conductivity of $CuAlO_2$, i.e. the electrons migrate in the direction of the illuminated side of the particle to react with adsorbed water and produce H_2. In contrast, holes move in the opposite direction, i.e. they move to the particles dark side to convert adsorbed sulfide into a mixture of polysulfide $S_n{}^{2-}$. The elementary processes can be summarized as follows

$$CuAlO_2 + (h\nu) \rightarrow CuAlO_2(e^-, h^+) \quad (1)$$

$$CuAlO_2(e^-) + H_2O \rightarrow CuAlO_2 + (1/2)H_2 + OH^- \quad \text{(Illuminated side)} \quad (2)$$

$$CuAlO_2(h^+) + nS^{2-} \rightarrow CuAlO_2 + S_n{}^{2-} \quad \text{(Dark side)} \quad (3)$$

When TiO_2 is added to $CuAlO_2$ and the resulted system is submitted to visible light, only $CuAlO_2$ is activated. The processes taking place into $CuAlO_2$ remained the same as in the case of

pure material except that the produced electrons are injected into the conduction band of TiO_2 for reducing at their surface water into gaseous H_2 following to the processes:

$$CuAlO_2 + (h\nu) \rightarrow CuAlO_2(e^-, h^+)$$

$$CuAlO_2(e^-) + TiO_2 \rightarrow CuAlO_2 + TiO_2(e^-) \quad (4)$$

$$CuAlO_2(e^-, h^+) + TiO_2 \rightarrow CuAlO_2(h^+) + TiO_2(e^-) \quad (5)$$

$$TiO_2(e^-) + H_2O \rightarrow TiO_2 + (1/2)H_2 + OH^- \quad (6)$$

$$CuAlO_2(h^+) + nS^{2-} \rightarrow CuAlO_2 + S_n{}^{2-}$$

The main advantages of this heterojunction according to the high conversion efficiency obtained in this work are the following: (i) the conduction band of TiO_2 seems to be more well matched to E_{H_2O/H_2} than the conduction band of $CuAlO_2$ which favors the kinetic of electron transfer at the interface TiO_2/electrolyte; (ii) the difference of energy between the respective conduction band of each SC ($\delta E_\alpha E_{CB/CuAlO_2} - E_{CB/TiO_2} = 0.36$ eV) is traduced by a strong driving force for electron injection which leads to an improvement of charges separation and an increase of the charges carrier lifetime.

3.3. pH effect

The effect of the pH on the photocatalytic performance of this junction was realized using $S_2O_3{}^{2-}$ as hole scavenger instead of S^{2-}, $S_2O_3{}^{2-}$ exhibits a wide range of chemical stability against pH (5.5 < pH < 14). As observed in Fig. 7, an augmentation of pH increases the H_2 generation until a maximum value at pH ∼ 11, above which a drastic decreasing was observed. Considering that the electronic bands of $CuAlO_2$ are pH-insensitive, the pH effect can be attributed then essentially to the modification of TiO_2 band positions which are known to shift negatively with increasing pH by −0.059/pH. However, this behavior can have two controversial effects: in the first place, energy narrowing between the respective conduction band of each SC favors the

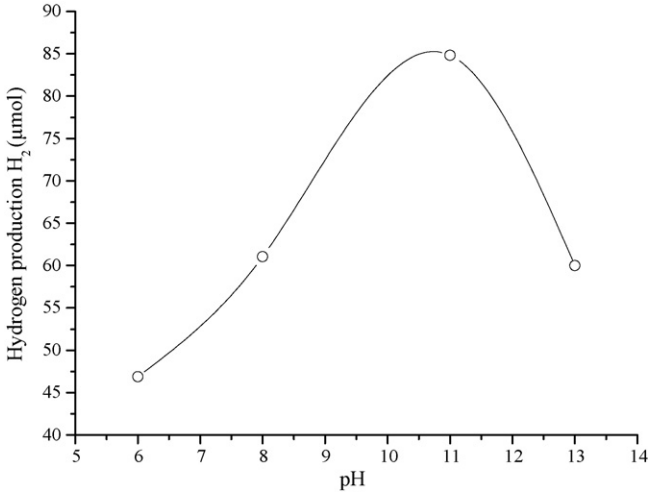

Fig. 7. pH dependence of H_2-evolution of $CuAlO_2$ (300 mg)/TiO_2 (75 mg) (optimal ratio) heterojunction in $S_2O_3{}^{2-}$ (0.025 M) electrolyte.

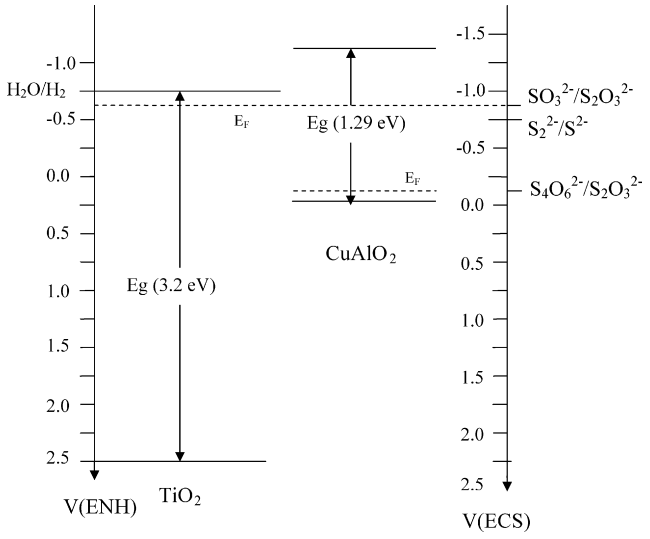

Fig. 8. Energy diagram of $CuAlO_2$/TiO_2 heterojunction at pH 13; the conduction and valence band of TiO_2 was established according to Mimming reports [22].

kinetic of electron transfer which is traduced by an increase of the photoactivity against pH. Furthermore, it leads to the decrease of the driving force (δE), which reduces the efficiency of physically charge separation. In any case, the maximal photoactivity for our system occurs at pH 11, which corresponds to the TiO_2 conduction band of −0.85 V/SCE and a δE value of 0.49 eV.

It should be noted at this stage that the reactivity of holes plays an important role in the heterojunctions application in photocatalysis. This fact is illustrated by the efficiency variation of the heterojunction when used in $S_2O_3{}^{2-}$ media instead of S^{2-} at the same pH value (∼13). Indeed, H_2 production in S^{2-} solution (5265 μmol) is very high compared to that obtained with $S_2O_3{}^{2-}$ (60 μmol) under similar condition. As it is well known, the oxidation of $S_2O_3{}^{2-}$ can generate mainly $S_4O_6{}^{2-}$ and/or $SO_3{}^{2-}$, identified in our case by plotting $J(V)$ curves of the obtained solution after a photocatalytic test (not presented here). The results, i.e. half-waves identification according to previous works [16] and the width of the inflection curves indicate that oxidation of $S_2O_3{}^{2-}$ by holes induces mainly the production of $S_4O_6{}^{2-}$ in our experimental conditions with a potential E^0 ($S_4O_6{}^{2-}/S_2O_3{}^{2-}$) of −0.16 V. Therefore, it could be reasonable to consider that the generated photovoltage in $S_2O_3{}^{2-}$ media is lower than that produced in S^{2-} solution (see the energetic diagram in Fig. 8). This fact influences directly the kinetic of holes reactivity, which increases with the photovoltage, and as a consequence, improves the charges separation. Because of that, the junction exhibited a better photoactivity in S^{2-} electrolyte.

4. Conclusion

An interesting approach to improve photocatalytic efficiency of the narrow band gap $CuAlO_2$ SC has been developed in the present work. $CuAlO_2$ was easily prepared and some of its physico-chemical properties were studied. Pure $CuAlO_2$ and $CuAlO_2$ loaded TiO_2 were applied to the H_2 production and sulfide and thiosulfate conversion into less harmful products such as $S_n{}^{2-}$ and $S_4O_6{}^{2-}$ under visible light irradiation. In the

ideal configuration $CuAlO_2$ (300 mg)/TiO_2 (75 mg) heterojunction showed efficiency six times greater than that of $CuAlO_2$ under the same experimental conditions. This activation was attributed to a better charge separation and an increase of electrons transfer ascribed to the strong driving force developed in the heterojunction. TiO_2 can be considered, in this case, an electron accumulator. The importance of the holes reactivity against the global process mechanism was studied using both S^{2-} and $S_2O_3{}^{2-}$ as reducing agents. The most important result is that the efficiency of the system was found to be highly dependent on the reactivity of holes, which leads to think that a judicious choice should be taken to select the suitable hole scavenger that results in high photovoltage. The fact that the energy bands of TiO_2 depend on the pH and that those of $CuAlO_2$ are insensitive was exploited to adjust the respective conduction bands for improving the efficiency. The suitable pH value of 11 has been determined. TiO_2 is cheap and has a high resistance to photocorrosion, which leads us to conclude that its use instead of noble metal related oxide represents a real alternative. The use $CuAlO_2$/TiO_2 heterojunction, in which the properties of each semiconductor is complementary to the other is attractive for the solar light conversion.

References

[1] A. Fujishima, K. Honda, Nature 238 (1972) 37–38.
[2] T. Bak, J. Nowotny, M. Rekas, C.C. Sorrell, Int. J. Hydrogen Energy 27 (2002) 991–1022.
[3] M. Ni, M.K.H. Leung, D.Y.C. Leung, K. Sumathy, Renew. Sust. Energ. Rev. 11 (2007) 401–425.
[4] J.A. Turner, Science 305 (2004) 972–974.
[5] J.A. Turner, Science 285 (1999) 687–689.
[6] M. Shokkumar, Int. J. Hydrogen Energy 23 (1998) 427–438.
[7] N. Koriche, A. Bouguelia, A. Aider, M. Trari, Int. J. Hydrogen Energy 30 (2005) 693–699.
[8] G.R. Bamwenda, S. Tsubota, T. Nakamura, M. Haruta, J. Photochem. Photobiol. A 89 (1995) 177–189.
[9] S. Sakthivel, M.V. Shankar, M. Palanichamy, B. Arabindoo, D.W. Bahnemann, V. Murugesan, Water Res. 38 (2004) 3001–3008.
[10] T. Sano, N. Negishi, D. Mas, K. Takeuchi, J. Catal. 194 (2000) 71–79.
[11] W. Siripala, A. Ivanovskaya, T.F. Jaramillo, S.H. Baeck, E.W. McFarland, Sol. Energy Mater. Sol. Cells 77 (2003) 229–237.
[12] Y. Bessekhouad, D. Robert, J.-V. Weber, Catal. Today 101 (2005) 315–321.
[13] Y. Bessekhouad, D. Robert, J.V. Weber, J. Photochem. Photobiol. A 163 (2004) 569–580.
[14] S.V. Tambwekar, D. Venugopal, M. Subrahmanyam, Int. J. Hydrogen Energy 24 (1999) 957–963.
[15] S. Saadi, A. Bouguelia, M. Trari, Renew. Energy 31 (2006) 2245–2256.
[16] M. Younsi, A. Aider, A. Bouguelia, M. Trari, Sol. Energy 78 (2005) 574–580.
[17] V. Kumar, T.P. Sharma, J. Phys. Chem. Solids 59 (1998) 1321–1325.
[18] F.A. Benko, F.P. Koffyberg, J. Phys. Chem. Solids 45 (1984) 57–59.
[19] A. Nozik, R. Memming, J. Phys. Chem. 100 (1996) 13061–13078.
[20] Y. Bessekhouad, M. Trari, J.P. Doumerc, Int. J. Hydrogen Energy 28 (2003) 43–48.
[21] M. Trari, A. Bouguelia, Y. Bessekhouad, Sol. Energy Mater. Sol. Cells 90 (2006) 190–202.
[22] R. Mimming, Electrochim. Acta 25 (1980) 77–88.